

1 **Title**

2 Analysis of the influence of thermal gradients inside T-history samples on the method  
3 accuracy: theoretical approach

4 **Authors**

5 Javier Mazo<sup>\*</sup>, Mónica Delgado, Ana Lázaro, Pablo Dolado, Conchita Peñalosa, José María  
6 Marín, Belén Zalba

7 Aragón Institute for Engineering Research (I3A), Thermal Engineering and Energy Systems  
8 Group, University of Zaragoza

9 Agustín Betancourt Building, C/María de Luna 3, 50018 Zaragoza, Spain,

10 Phone: (+34) 876 555 584, *\*Corresponding email: jmazo@unizar.es*

11 **Abstract**

12 The present work analyses the effect of radial thermal gradients inside T-history samples on  
13 the enthalpy temperature curve measurement. A conduction heat transfer model has been  
14 utilized for this purpose. Some expressions have been obtained that relate the main  
15 dimensionless numbers of the experiments with the deviations in specific heat capacity, phase  
16 change enthalpy and phase change temperature estimations. Although these relations can only  
17 be strictly applied to solid materials (e.g. measurements of shape stabilized phase change  
18 materials, SSPCM), they can provide some useful and conservative bounds for the deviations  
19 of the T-history method. Biot numbers emerge as the most relevant dimensionless parameters  
20 in the accuracy of the specific heat capacity and phase change enthalpy estimation whereas  
21 this model predicts a negligible influence of the temperature levels used for the experiments  
22 or the Stefan number.

23 **Keywords:** T-history method, Phase Change Material, Enthalpy, Storage Capacity

24 **Nomenclature**

A	Time integral of $T_{\infty}-T_{sur}$ [K·s]	$\delta T_m$	Error in phase change temperature [°C]
$\hat{A}$	Measured time integral of $T_{\infty}-T_{sur}$ [K·s]	$\theta$	Dimensionless temperature
Bi	Biot number	$\lambda$	Thermal conductivity [W/(m·K)]
C	Thermal capacity [J/K]	$\xi$	Eigenvalue of cond. heat transfer problem
$\hat{C}$	Measured thermal capacity [J/K]	$\rho$	Density [kg/m <sup>3</sup> ]
$c_p$	Specific heat capacity [J/(kg·K)]	<b>Abbreviations</b>	
e	Thickness of the tube [m]	DSC	Differential Scanning calorimetry
$e_q$	Relative error in surface temperature	PCM	Phase Change Material
$e_{\bar{T}}$	Error in the sample average temperature	SSPCM	Shape Stabilized Phase Change Material
f	Liquid fraction	<b>Subscripts</b>	
h	Enthalpy [kJ/(kg·K)], heat transfer coefficient [W/(m <sup>2</sup> ·K)]	0	Initial conditions
$J_0$	Zeroth order Bessel function	cn	Measured in the centreline of the sample
$J_1$	First order Bessel function	e	Relative to the T-history experiment
$L_c$	Characteristic length [m]	m	Relative to the melting process
m	Mass [kg]	ms	Relative to a measured temperature
R	Radius [m], thermal resistance [K·m <sup>2</sup> /W]	r-c	Combined radiation and convection
$r_e$	Relation between temperature errors	ref	Relative to the reference sample
Ste	Stefan number	s	Relative to a T-history sample
T	Temperature [°C]	sur	Relative to the surface of the tube
t	Time [s]	t	Relative to the tube
<b>Greek symbols</b>		$\infty$	Ambient temperature

$\Delta T_m$  Phase change temperature range [°C]

25 **1. Introduction**

26 The determination of the thermo-physical properties of phase change materials is essential

27 both for the correct design of thermal energy storage systems and for their simulation. The

28 enthalpy versus temperature curve determination (h-T) is therefore crucial. Although the DSC  
29 technique is the most commonly used for this determination, the T-history method is currently  
30 attracting increasing attention due to its simplicity and its good results [1]. In light of the  
31 results of previous experimental works dealing with the evaluation of the accuracy of the T-  
32 history method, such as that of Lazaro et al. [2] on the empirical verification of a T-history set  
33 up, researchers [2-3] generally agree on the suitability of this methodology for measuring the  
34 enthalpy temperature curve in a typical PCM application.

35 The T-history method assumes a uniform temperature distribution inside the samples. In order  
36 to ensure this condition, the restriction for the lumped capacitance systems ( $Bi=h \cdot L_c/\lambda < 0.1$ )  
37 has been used [4]. This restriction is based on the analysis of classical transient heat  
38 conduction problems, where the phase change process is not considered. In this restriction,  
39 different definitions can be used for the characteristic length: the ratio between volume and  
40 heat transfer area or the distance corresponding to the highest temperature gradient. Some  
41 researchers [5-7] have used the first expression ( $Bi=h \cdot R/(2 \cdot \lambda)$ ), whereas the second and more  
42 conservative one ( $Bi=h \cdot R/\lambda$ ) has been utilized in [8-10].

43 Hong et al. [9] claimed that the classical condition for the Biot number was not sufficient for  
44 ensuring a uniform temperature distribution during the phase change process. They measured  
45 radial thermal gradients inside a sodium acetate sample ( $R=8\text{mm}$ ) during its cooling process.  
46 Temperature differences during its solidification were higher than those corresponding to the  
47 sensible heat transfer stages. They found that more accurate calculations were obtained when  
48 the temperature of the centreline was used. However, since a qualitative explanation of this  
49 fact was not found, they suggested that an analytical investigation of the effect on h-T  
50 calculations of these thermal gradients would be interesting. The objective of the present  
51 study is to analyse the influence of radial thermal gradients inside the T-history samples on  
52 the deviations of the calculated h-T curve.

53        **2. Methodology**

54    For this purpose, the thermal gradients inside T-history samples resulting from conduction  
55    heat transfer are evaluated. Only radial temperature distribution is considered, since T-history  
56    tubes are usually designed with a large ratio between their length and diameter ( $L/D > 10$ ).  
57    Hong et al. [9] and Rady et al. [11] have empirically proved that axial thermal gradients are  
58    negligible during the experiments. Two approaches have been followed: first, an analytical  
59    model allows a prediction of the deviation in heat capacity measurements and, secondly, a  
60    numerical model has been used in order to evaluate these effects when the phase change  
61    process takes place. Dimensionless analysis has been used with the objective of obtaining  
62    general relations between the conditions of the T-history experiments and the deviations in h-  
63    T curve calculations.

64        **2.1 General assumptions**

65    In this work, only conduction heat transfer is considered and therefore the influence of natural  
66    convection during the phase change process or the effect of movement of the solid phase  
67    during the melting or solidification process are not taken into account. Additionally, it has  
68    been assumed that the cylindrical section of the sample holder is completely filled by the  
69    PCM and reference material. For these reasons, the results can only strictly be applied to the  
70    measurements of Shape Stabilized PCM (SSPCM) where a solid material is used for the  
71    reference sample. The use of the T-history method for the evaluation of the h-T curves of  
72    these solid PCM composites is very promising. For example, Rady et al. [11] applied this  
73    method for the thermal characterization of PCM granules and Palomo and Dauvergne [12]  
74    developed an experimental methodology similar to T-history –in terms of sample geometry  
75    and thermal excitation- that allowed the complete thermodynamic characterization of SSPCM  
76    by means of a mathematical inverse method analysis.

77

78 Considering the particular phenomena that take place during the phase change process,  
 79 researchers have used different designs for the sample holders in order to control them with  
 80 the aim of approaching the ideal case of uniform radial melting or solidification. For  
 81 instance, horizontal tubes have been used in [2, 13] thus minimizing the axial displacement of  
 82 the solid phase. Additionally, Hong et al. [8] located a stainless wire in the centre of the  
 83 sample in order to prevent the ice from floating. With the objective of ensuring that the tubes  
 84 remain filled during the experiment, a vertical volume expansion buffer was used by Peck et  
 85 al. [13]. When extrapolating the results of this study to a particular T-history experimental set  
 86 up, the importance of these effects has to be considered.

87 On the other hand, the influence of natural convection during the melting process can be  
 88 evaluated using the correlation of Raithby and Hollands [14]. For the thermal gradients  
 89 calculated in this work or experimentally measured by Hong et al. [9], a relation between the  
 90 effective and liquid thermal conductivity of near 1.5 can be obtained. Therefore, for a general  
 91 case, the results from this study can be taken as a conservative estimation of the maximum  
 92 errors due to the radial thermal gradients inside the T-history tubes.

93 Additionally, with the aim of simplifying the dimensionless analysis of the problem, thermal  
 94 conductivity and heat capacity of the liquid and solid phases are considered equal and a  
 95 constant equivalent convective and radiant coefficient is assumed ( $h_{r-c}$ ). In this work sub-  
 96 cooling and hysteresis are not taken into account.

## 97 **2.2 Dimensionless numbers**

98 Assuming these simplifications, the heat transfer problem of the PCM sample can be  
 99 represented by the following equations (1)-(6). An analogous formulation can be applied to  
 100 the reference sample.

$$101 \quad \rho_{PCM} \cdot \left( c_{p,PCM} \cdot \frac{\partial T_{PCM}}{\partial t} + h_m \cdot \frac{\partial f}{\partial t} \right) = \frac{\lambda_{PCM}}{r} \cdot \frac{\partial}{\partial r} \left( r \cdot \frac{\partial T_{PCM}}{\partial r} \right) \quad 0 \leq r \leq R - e \quad (1)$$

$$102 \quad \lambda_{PCM} \cdot \frac{\partial T_{PCM}}{\partial r} \Big|_{r=R-e} = \lambda_t \cdot \frac{\partial T_t}{\partial r} \Big|_{r=R-e} \quad (2)$$

$$103 \quad \rho_t \cdot c_{p,t} \cdot \frac{\partial T_t}{\partial t} = \frac{\lambda_t}{r} \cdot \frac{\partial}{\partial r} \left( r \cdot \frac{\partial T_t}{\partial r} \right) \quad R - e < r \leq R \quad (3)$$

$$104 \quad \lambda_t \cdot \frac{\partial T_t(R,t)}{\partial r} = h_{r-c} \cdot (T_\infty - T_t(R,t)) \quad (4)$$

$$105 \quad T_{PCM}(r, t = 0) = T_0 \quad 0 \leq r \leq R - e \quad (5)$$

$$106 \quad T_t(r, t = 0) = T_0 \quad R - e < r \leq R \quad (6)$$

107 According to these conduction heat transfer problems, a set of dimensionless numbers has  
 108 been defined for the analysis, shown in the following table (table 1). The range of variation  
 109 for each dimensionless number is also presented. These values have been determined  
 110 according to the typical thermal properties and experimental conditions used in the T-history  
 111 method.

112 **Table 1.** Dimensionless numbers used in this study. In brackets values for the base case.

Dimensionless number	Range of variation	Dimensionless number	Range of variation
$Bi_{ref} = \frac{h_{r-c} \cdot R}{\lambda_{ref}}$	[0-0.2] (0.05)	$Ste = \frac{c_{p,PCM} \cdot (T_\infty - T_m)}{h_m}$	[0.1-1] (0.3)
$C_{r,ref} = \frac{m_{ref} \cdot c_{p,ref}}{m_{ref} \cdot c_{p,ref} + m_t \cdot c_{p,t}}$	[0.5-0.9] (0.85)	$R_t/R_{r-c} = \frac{\lambda_t}{h_{r-c} \cdot e}$	[0-0.005] (0.003)
$Bi_{PCM} = \frac{h_{r-c} \cdot R}{\lambda_{PCM}}$	[0-0.2] (0.15)	$\theta_m = \frac{\Delta T_m}{T_\infty - T_m}$	[0.02-0.16] (0.08)
$C_{r,PCM} = \frac{m_{PCM} \cdot c_{p,PCM}}{m_{PCM} \cdot c_{p,PCM} + m_t \cdot c_{p,t}}$	[0.5-0.9] (0.7)	$\theta_e = \frac{T_\infty - T_m}{T_\infty - T_0}$	[0.3-0.7] (0.06)

113

### 114 **2.3 Analytic model: estimation of deviation in specific heat**

115 A simplified model is proposed for the analytic estimation of the deviation in the specific heat  
 116 capacity calculation. In this model the following additional assumptions are made:

117 -no latent heat is considered;

118 -the container is considered as a lumped heat capacity system: this simplification can be

119 acceptable if  $\frac{\lambda_s}{\rho_s \cdot c_{p,s} \cdot (R-e)^2} \ll \frac{\lambda_t}{\rho_c \cdot c_{p,t} \cdot e^2}$  and  $h_{r-c} \ll \frac{\lambda_t}{e}$

120 According to these assumptions, the transient conduction heat transfer problem corresponding  
 121 to each sample can be represented by a single domain formulation (equations (7)-(8)). If this  
 122 is compared to the classical problem of transient conduction heat transfer in cylinders [4],  
 123 only one additional term –the heat capacity of the tube- is introduced into the boundary  
 124 condition equation (equation (8)).

$$125 \quad \rho_s \cdot c_{p,s} \cdot \frac{\partial T_s}{\partial t} = \frac{\lambda_s}{r} \cdot \frac{\partial}{\partial r} \left( r \cdot \frac{\partial T_s}{\partial r} \right) \quad 0 \leq r \leq R - e \quad (7)$$

$$126 \quad -\lambda_t \cdot \frac{\partial T_s(R-e,t)}{\partial r} + h_{r-c} \cdot \frac{R}{R-e} (T_\infty - T_s(R - e, t)) = \frac{m_t \cdot c_{p,t}}{2\pi \cdot (R-e)} \cdot \frac{\partial T_s(R-e,t)}{\partial t} \quad (8)$$

127 Similarly to the classical transient heat transfer problems, the solutions can be expressed using  
 128 a function series (equation (9)). In the following calculations, the first term approximation  
 129 will be used.

$$130 \quad T(r, t) \approx T_\infty - (T_\infty - T_0) \cdot \sum_{i=1}^{\infty} C_i \cdot J_0 \left( \frac{\xi_i \cdot r}{R-e} \right) \cdot e^{-\frac{\xi_i^2 \cdot \lambda_s}{\rho \cdot c_{p,s} \cdot (R-e)^2} \cdot t} \quad (9)$$

131 where  $\xi_i$  are the infinite solutions of the transcendental equation (equation (10)).

$$132 \quad 2 \cdot \frac{J_1(\xi_i) \cdot \xi_i}{J_0(\xi_i)} + \xi_i^2 \cdot \frac{m_t \cdot c_{p,t}}{m_s \cdot c_{p,s}} = 2 \cdot Bi \quad (10)$$

133 For low numbers of the Biot number, Bessel functions can be truncated in order to simplify  
 134 the solution. Therefore, the transcendental equation (equation (10)) can be approximated by  
 135 equation (11), expressed in terms of the Biot number and relative heat capacity of the sample  
 136 ( $C_r$ , defined in table 1), for the calculation of the first eigenvalue of the problem ( $\xi_1$ ).

$$137 \quad \xi_1^2 \approx \frac{2 \cdot Bi}{\left(1 + \frac{m_t \cdot c_{p,t}}{m_s \cdot c_{p,s}}\right)} = 2 \cdot Bi \cdot C_r \quad (11)$$

138 The exact thermal energy balance equation on which the T-history method is based is  
 139 equation (12). This equation can be modified in order to consider the measured temperature  
 140 ( $T_{ms}$ ) (equation (13)) using the relative errors ( $e_q$ ,  $e_{\bar{T}}$ ) associated to the surface temperature  
 141 and the average sample temperature which are defined in equations (14) and (15). These heat  
 142 balance equations (equations (12) and (13)) are formulated in a differential form. Similar

143 expressions were used by Moreno-Alvarez et al. [15] in their proposed differential analysis  
 144 method for the temperature evolutions measured by the T-history method.

$$145 \quad C_c \cdot \frac{d\bar{T}_s}{dt} + C_s \cdot \frac{dT_t}{dt} = \bar{h} \cdot A \cdot (T_\infty - T_{sur}) \quad (12)$$

$$146 \quad C_c \cdot \frac{dT_{ms}}{dt} \cdot (1 + e_{\bar{T}}) + C_s \cdot \frac{dT_{ms}}{dt} \cdot (1 + e_q) = \bar{h} \cdot A \cdot (T_\infty - T_{ms}) \cdot (1 + e_q) \quad (13)$$

$$147 \quad e_{\bar{T}} = \frac{T_{ms} - \bar{T}_s}{T_\infty - T_{ms}} \quad (14)$$

$$148 \quad e_q = \frac{T_{ms} - T_{sur}}{T_\infty - T_{ms}} \quad (15)$$

149 For low values of the Biot number, the errors in surface and average temperatures can be  
 150 approximated (equations (16) and (17)). Here, it has been considered that the temperature is  
 151 measured in the centreline of the cylinder. Similarly, analogous expressions can be obtained if  
 152 the temperature is measured at the surface.

$$153 \quad 1 + e_{\bar{T}} = \frac{T_\infty - \bar{T}_s}{T_\infty - T_{ms}} = 2 \cdot \frac{J_1(\xi_1)}{\xi_1} \approx 1 - \frac{\xi_1^2}{8} = 1 - \frac{Bi}{4} \cdot C_r \quad (16)$$

$$154 \quad 1 + e_q = J_0(\xi_1) \approx 1 - \frac{\xi_1^2}{4} = 1 - \frac{Bi}{2} \cdot C_r \quad (17)$$

155 The following equations represent the approximated method for obtaining the heat capacity of  
 156 the measured material (equation (18)) and the exact formulation –taking into account 1D heat  
 157 conduction effects- using the previously defined errors ( $e_{\bar{T}}$ ,  $e_q$ ) (equation (19)).

$$158 \quad \hat{C}_s + C_c = (C_{ref} + C_t) \cdot \frac{\int (T_\infty - T_{ms,s}) \cdot dt}{\int (T_\infty - T_{ms,ref}) \cdot dt} = (C_{ref} + C_t) \cdot \frac{\hat{A}_s}{\hat{A}_{ref}} \quad (18)$$

$$159 \quad C_s \cdot (1 + e_{\bar{T},s}) + C_t \cdot (1 + e_{q,s}) = [C_{ref} \cdot (1 + e_{\bar{T},ref}) + C_t \cdot (1 + e_{q,ref})] \cdot \frac{\hat{A}_s}{\hat{A}_{ref}} \cdot \frac{1 + e_{q,s}}{1 + e_{q,ref}} \quad (19)$$

160 where  $\hat{C}_s$  is the measured heat capacity of the sample and  $\hat{A}_s$  and  $\hat{A}_{ref}$  the time integrated  
 161 difference between ambient and measured temperature of each material (sample and  
 162 reference). The following relation (equation (20)) between temperature measurement  
 163 deviations can be defined in order to obtain a more compact expression. It is important to note  
 164 that this relation is the same whether the temperature is measured at the surface or in the  
 165 centreline of the T-history samples.



166 
$$r_e = \frac{1+e_{\bar{r}}}{1+e_q} \approx \frac{1-\frac{Bi}{4} \cdot C_r}{1-\frac{Bi}{2} \cdot C_r} \quad (20)$$

167 Dividing equations (18) and (19), an expression for the deviation of specific heat capacity  
 168 ( $e_{cp}$ ), defined in equation (21), can be obtained. This relation between equation (18) and (19)  
 169 (equation (22)), can be thus expressed (equation (23)) in terms of the ratio of temperature  
 170 measurement errors ( $r_e$ ), the relative heat capacities of the samples ( $C_{r,i}$ ) and the relative error  
 171 in heat capacity ( $e_{cp}$ ).

172 
$$e_{cp} = \frac{\hat{C}_s - C_s}{C_s} \quad (21)$$

173 
$$\frac{\hat{C}_s + C_t}{C_s \cdot r_{e,s} + C_t} = \frac{C_{ref} + C_t}{C_{ref} \cdot r_{e,ref} + C_t} \quad (22)$$

174 
$$\frac{e_{cp} \cdot C_{r,s} + 1}{C_{r,s} \cdot (r_{e,s} - 1) + 1} = \frac{1}{C_{r,ref} \cdot (r_{e,ref} - 1) + 1} \quad (23)$$

175 From equation (23), an explicit formulation for the relative deviation in heat capacity can be  
 176 obtained (equation (24)).

177 
$$e_{cp} = \frac{C_{r,s} \cdot (r_{e,s} - 1) - C_{r,ref} \cdot (r_{e,ref} - 1)}{C_{r,s} \cdot [C_{r,ref} \cdot (r_{e,ref} - 1) + 1]} \quad (24)$$

178 Finally, if the above-mentioned approximation of  $r_e$  for low Biot numbers is assumed  
 179 (equation (20)) and the first terms of the Taylor series (developed from variables  $Bi_i \cdot C_{r,i}$ ) of  
 180 equation (24) are taken, a simplified expression for the deviation of the heat capacity  
 181 measurement can be obtained.

182 
$$e_{cp,s} \approx \frac{1}{4} \cdot \left( C_{r,s} \cdot Bi_s - \frac{C_{r,ref}^2}{C_{r,s}} Bi_{ref} \right) \quad (25)$$

183 It should be noted that this analytical model predicts the same deviation in the heat capacity  
 184 estimation whether the temperature of the samples is measured in their centreline or on their  
 185 surface, since the relation  $r_e$  is identical for both cases. Using equation (25), a maximum  
 186 deviation of 6% in the specific heat estimation can be obtained if the Biot number limit  
 187 ( $Bi = h \cdot R / (2 \cdot \lambda) = 0.1$ ) is considered.

188

189        **2.4 Numerical model**

190    A finite difference scheme has been developed for calculating conduction heat transfer inside  
191    the samples during the phase change process, where the phase change is formulated using the  
192    enthalpy method. The spatial mesh is uniformly distributed and a fully implicit method is  
193    used for time discretization. A spatial resolution of 0.2 mm and a time step of 10s have been  
194    used. The h-T curve is described in the simulations by an analytical function (equation (26)).  
195    Palomo et al. [12] have already used this analytical equation in the numerical study of their  
196    experimental methodology.

197    
$$h(T) = c_p \cdot (T - T_o) + \frac{1}{2} \cdot h_m \cdot \left[ 1 + \tanh \left( \frac{4 \cdot (T - T_m)}{\Delta T_m} \right) \right] \quad (26)$$

198        **2.4.1 Analysis of the errors**

199    The results of the numerical model have been integrated following the methodology proposed  
200    by Marín et al. [6]. Other researchers have proposed alternative algorithms in order to obtain  
201    the enthalpy-temperature curve from experimental data. Kravvaritis et al. [16] proposed what  
202    they called the “thermal delay method” which was based on a comparison of the heat balance  
203    equations corresponding to both samples during the same time interval. On the other hand,  
204    Moreno-Alvarez et al. [15] proposed a differential method considering the instantaneous  
205    temperature change rate of each material. It should be noted that under the assumptions of the  
206    proposed model for the analysis –the constant heat transfer coefficient ( $h_{r-c}$ )-, the obtained  
207    enthalpy temperature curve is the same whichever of these methods is applied.

208    A constant temperature increment has been taken for the integration. This temperature  
209    increment (0.1°C) is lower than the melting temperature range and much higher than the  
210    numerical precision of the calculated temperatures. The accuracy of the integration method  
211    has been verified for all cases by comparing the original analytical enthalpy-temperature  
212    curve with the numerical table obtained from the exact formulation (considering real  
213    temperatures of each material, equation (12)). The errors attributable to this numerical

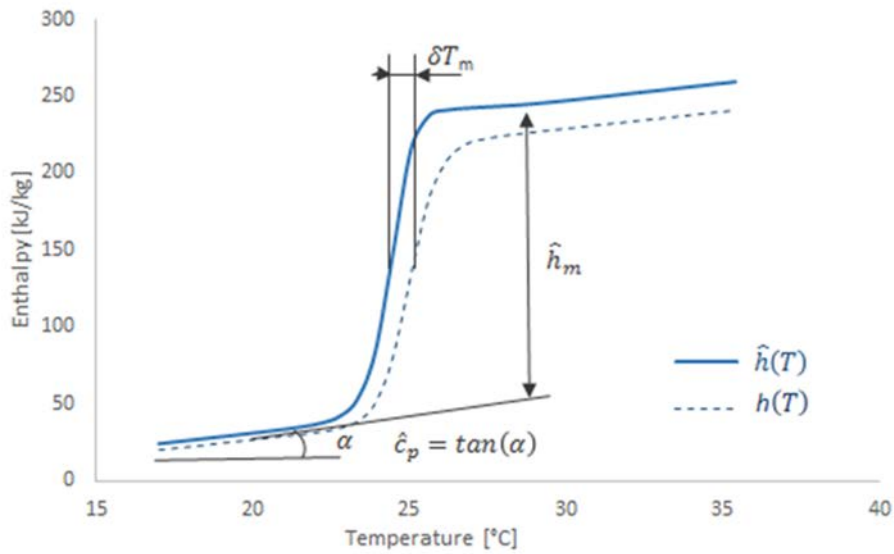
214 integration of the results are lower than 0.001% in the enthalpy estimation and smaller than  
 215 0.001°C in the phase change temperature measurement.

216 The resulting h-T curve is compared with the original analytical function. Three main  
 217 parameters have been identified in this study:  $c_p$ ,  $h_m$  and  $T_m$ . In figure 1 a representation of  
 218 these parameters is shown. Equations (21) and (27) define the relative errors in specific heat  
 219 and enthalpy that are analysed in the following sections. Since the shape of the calculated h-T  
 220 can vary from the original one, an average error in melting temperature is calculated with  
 221 equation (28) and made dimensionless by using equation (29).

$$222 \quad e_{h_m} = \frac{\hat{h}_m - h_m}{h_m} \quad (27)$$

$$223 \quad \delta T_m = \frac{\int_{f=0.1}^{f=0.9} (\hat{T}_{PCM}(f) - T_{PCM}(f)) \cdot df}{0.8} \quad (28)$$

$$224 \quad e_{\delta T_m} = \frac{\delta T_m}{(T_\infty - T_m)} \quad (29)$$



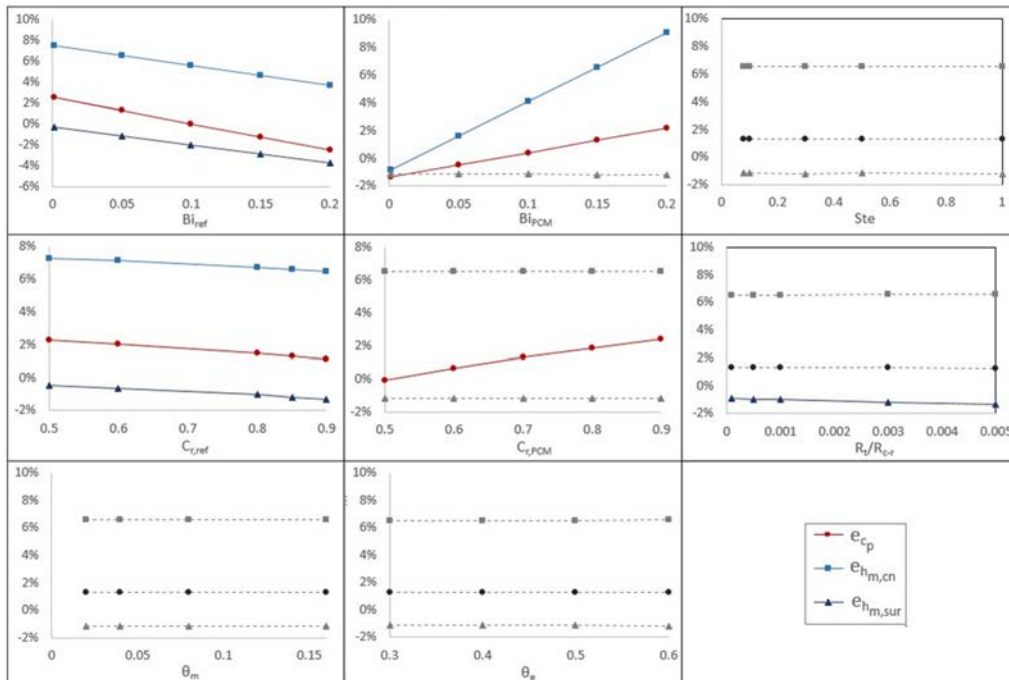
225  
 226 **Figure 1.** Graphical representation of the analysed parameters

227

228 **3. Results**

229 **3.1 Parametric analysis**

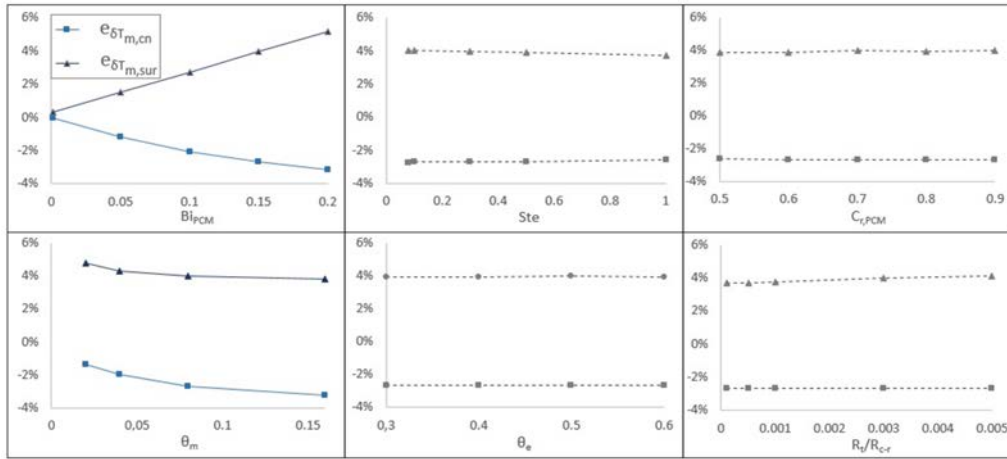
230 A first parametric analysis has been made in order to identify the dimensionless variables that  
 231 influence the errors defined in the previous section. In this analysis each dimensionless  
 232 variable has been independently modified within the range shown in Table 1 –while the rest  
 233 of the variables remain at the fixed values shown in the same table. The influence of each  
 234 independent dimensionless variable on the deviations is plotted in figures 2 and 3. The  
 235 influences that are considered relevant in this study are highlighted with a continuous line.  
 236 This analysis shows  $Bi$  and  $C_r$  as the most relevant numbers for the calculation of  $e_{cp}$  and  $e_{hm}$ .  
 237 Considering the error in the phase change temperature estimation ( $e_{\delta T_m}$ ), the most influential  
 238 variables are  $Bi_{PCM}$  and the dimensionless temperature  $\theta_m$ . As predicted by the previously  
 239 defined analytical model, the estimation of the heat capacity is the same whether the  
 240 temperature is measured at the surface of the tube or in the centreline.



241

242

**Figure 2.** Parametric analysis of the errors.

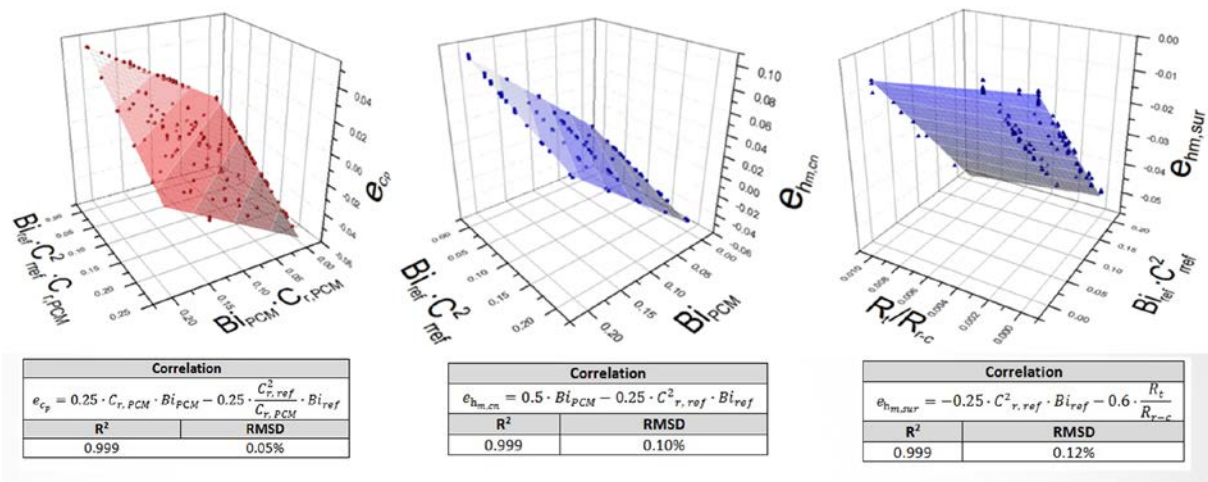


243

244 **Figure 3.** Parametric analysis of the errors in phase change temperature measurement.

245 **3.2 Interaction between dimensionless variables**

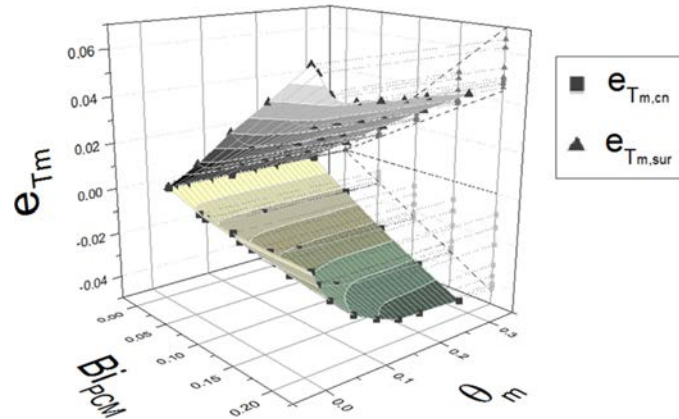
246 Secondly, the interaction of the influential dimensionless variables identified in the previous  
 247 parametric analysis has been investigated. First of all, the influence of different combinations  
 248 of  $Bi_{PCM}$ ,  $Bi_{ref}$ ,  $C_{r,PCM}$  and  $C_{r,ref}$  on the estimation of  $c_p$  and  $h_m$  has been analysed. In the case of  
 249 the estimation of the phase change enthalpy when the temperature is measured at the surface,  
 250 the influence of  $R_i/R_{r-c}$  has also been analysed. The correlations obtained from this analysis  
 251 are plotted in figure 4. They show a good fit to the calculated deviations. Furthermore, the  
 252 correlation for the error in the specific heat capacity estimation is the same as the expression  
 253 predicted by the analytical approach.



254

255

**Figure 4.** Correlations obtained from the study.



257

258 **Figure 5.** Influence on the phase change temperature of Biot number and  $\theta_m$ 

259 As can be seen in figure 5, a more complex relation has been found between the Biot number  
 260 of the PCM sample and the dimensionless temperature  $\theta_m$  with the error in the phase change  
 261 temperature measurement. If a melting T-history experiment is considered, the phase change  
 262 temperature is always overestimated when the temperature is measured at the surface whereas  
 263 the opposite effect is observed if the temperature of the centreline is used. For low values of  
 264  $\theta_m$  (corresponding to materials with a narrower phase change temperature range), the error is  
 265 reduced if the centreline temperature is taken and increased if the surface temperature is  
 266 considered. Some useful simplified relations can be extracted from this analysis in order to  
 267 provide some bounds for these errors (equations (30)-(31)).

$$268 \quad -0.22 \cdot Bi_{PCM} \leq \frac{(T_\infty - T_m) \cdot \delta T_{m,c}}{|T_\infty - T_m|^2} \leq 0 \quad (30)$$

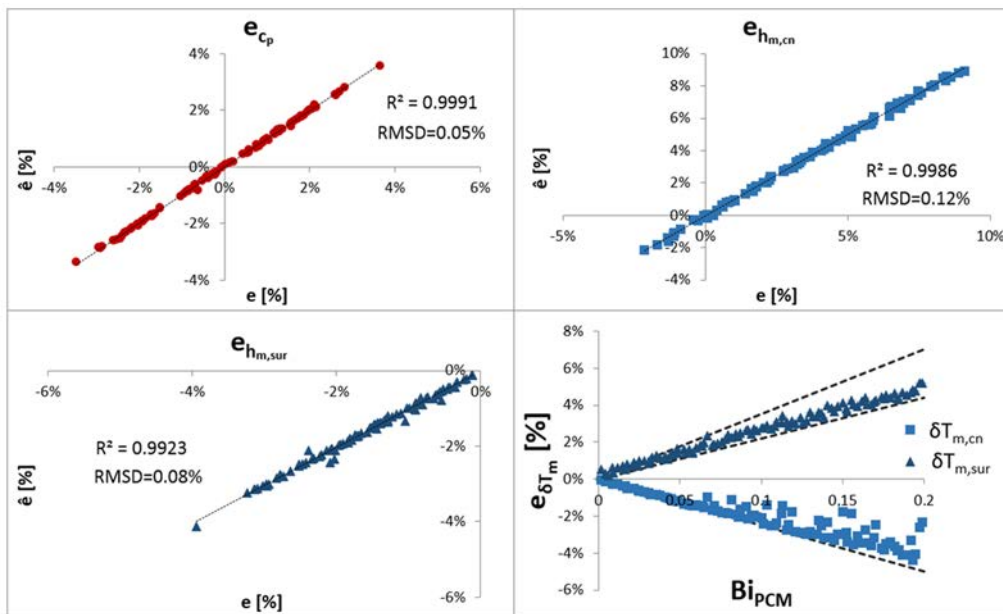
$$269 \quad 0.22 \cdot Bi_{PCM} \leq \frac{(T_\infty - T_m) \cdot \delta T_{m,s}}{|T_\infty - T_m|^2} \leq 0.35 \cdot Bi_{PCM} \quad (31)$$

### 270 **3.3 Analysis of the correlations obtained over a sample of the whole space of**

#### 271 **dimensionless numbers**

272 The expressions obtained for the error estimations are based on a correlation over a sample  
 273 space where only the “active” dimensionless numbers are varied. However, in this analysis  
 274 the influence of some dimensionless numbers may have remained concealed. Therefore, the

275 correlations have been tested and verified within a more representative sample of the input  
 276 variable space (defined in table 1). Since the number of input variables is high, a Montecarlo  
 277 based sampling method has been used for this purpose. A sample of 100 cases has been  
 278 obtained using Latin Hypercube (LH) Sampling [17], where each dimensionless number has  
 279 been considered as a uniformly distributed random variable over the intervals defined in table  
 280 1. The previously obtained relations for the errors are compared to the results corresponding  
 281 to the Montecarlo sample. As can be seen in figure 6, these relations fit these numerical  
 282 results: the maximum root-mean-square deviation (RMSD) is 0.12% and the worst coefficient  
 283 of determination is 0.992.



284  
 285 **Figure 6.** Comparison of the relations obtained with the results over the LH sample.

286 **4. Conclusions**

287 The effect of radial conduction heat transfer inside T-history samples on the deviations  
 288 produced in the h-T curve evaluation has been analysed. In this study, the measurement of  
 289 temperature in the centreline of the sample and at its surface has been taken into account. The  
 290 errors have been quantified and some useful relations have been obtained between the

291 dimensionless numbers that define the experiments and the errors produced in heat capacity,  
292 phase change enthalpy and temperature (table 2).

293 According to the results of the analysed heat transfer model, the deviation of heat capacity  
294 and phase change enthalpy does not depend on the Stefan number and temperature levels of  
295 the experiment (related to  $\theta_m$  and  $\theta_c$ ). The difference between the Biot numbers corresponding  
296 to the PCM and the reference substance is the most important contribution to the deviation of  
297 the heat capacity estimation, whereas the Biot number of the PCM sample is the most relevant  
298 dimensionless variable in the phase change enthalpy evaluation if the temperature is measured  
299 in the centreline. Considering the heat capacity estimation, the same results are obtained  
300 whether the temperature is measured in the centreline or at the surface of the sample. A lower  
301 error in phase change enthalpy is obtained if the temperature is measured at the surface.

302 Furthermore, this error does not depend on the PCM thermo-physical properties. However,  
303 this temperature measure produces a higher deviation in the phase change temperature  
304 estimation, especially when testing pure substances or materials with a narrow phase change  
305 temperature range.

306 As previously mentioned, the results of this study can only be strictly applied to T-history  
307 experiments with SSPCM where a solid material is used as the reference sample. In these  
308 cases, the relations obtained can be utilized to size the samples, to determine the favourable  
309 experimental conditions and to calibrate or correct the results. Calibration of the T-history is  
310 an interesting method for improving the accuracy of the measurements. For instance,  
311 Rathgeber et al. [18] applied a calibration to the heat capacity and phase change enthalpy  
312 measured values based on the characterization of reference materials that produced an  
313 improved agreement with DSC results.

314



315 **Table 2.** Correlations and bounds for T-history deviations owing to radial conduction

Correlation	Bounds for $T_m$ deviations
$e_{c_p} = 0.25 \cdot C_{r,PCM} \cdot Bi_{PCM} - 0.25 \cdot \frac{C_{r,ref}^2}{C_{r,PCM}} \cdot Bi_{ref}$	
$e_{h_{m,cn}} = 0.5 \cdot Bi_{PCM} - 0.25 \cdot C_{r,ref}^2 \cdot Bi_{ref}$	$-0.22 \cdot Bi_{PCM} \leq \frac{(T_\infty - T_m) \cdot \delta T_{m,cn}}{ T_\infty - T_m ^2} \leq 0$
$e_{h_{m,sur}} = -0.25 \cdot C_{r,ref}^2 \cdot Bi_{ref} - 0.6 \cdot \frac{R_t}{R_{r-c}}$	$0.22 \cdot Bi_{PCM} \leq \frac{(T_\infty - T_m) \cdot \delta T_{m,sur}}{ T_\infty - T_m ^2} \leq 0.35 \cdot Bi_{PCM}$

316

317 The extrapolation of these results to a general case of T-history measurement has to be done  
318 carefully: the similarity of each particular case to the main assumptions of the analysed model  
319 has to be revised (free convection and solid PCM movement inside the sample being  
320 neglected, having a fully filled section). However, considering free convection effects, the  
321 analysed heat conduction model overestimates thermal gradients inside the samples. Since it  
322 produces a conservative estimation of the deviations, the relations obtained can be used in  
323 order to establish some bounds for these errors. For example, if the temperature is measured  
324 inside the sample the following relations (equations (32)-(34)) can be applied. These can be  
325 useful to complete the classical restriction for the Biot number since they relate some  
326 parameters associated with the experimental conditions to the accuracy of the method.  
327 Considering these relations, the more restrictive Biot conduction ( $Bi=h \cdot R/\lambda < 0.1$ ) is  
328 recommended in order to ensure that the deviations in heat capacity and phase change  
329 enthalpy measurements are lower than 5%.

330 
$$e_{c_p} \leq 0.25 \cdot C_{r,PCM} \cdot Bi_{PCM} \tag{32}$$

331 
$$e_{h_{m,c}} \leq 0.5 \cdot Bi_{PCM} \tag{33}$$

332 
$$-0.22 \cdot |T_\infty - T_m| \cdot Bi_{PCM} \leq \delta T_{m,c} \cdot \frac{(T_\infty - T_m)}{|T_\infty - T_m|} \leq 0 \tag{34}$$

333

334 **Acknowledgments**

335 The authors would like to thank the Spanish government for partially funding this work  
336 within the framework of research projects (MICINN-FEDER): ENE2011-28269-C03-01,  
337 ENE2011-22722 and ENE2014-57262-R.

338 **References**

- 339 [1] Solé A, Miró L, Barreneche C, Martorell I and Cabeza L F 2013 Review of the T-history  
340 method to determine thermophysical properties of phase change materials (PCM) *Renew.*  
341 *Sust. Energ. Rev.* 26 425-36.
- 342 [2] Lazaro A, Günther E, Mehling H, Hiebler S and Zalba B 2006 Verification of a T-history  
343 installation to measure enthalpy versus temperature curves of phase change materials *Meas.*  
344 *Sci. Technol.* 17 2168-74
- 345 [3] Günther E, Hiebler S, Mehling H and Redlich R 2009 Enthalpy of phase change material  
346 as a function of temperature: required accuracy and suitable measurement methods, *Int. J.*  
347 *Thermophys.* 30 1257-69
- 348 [4] Incropera F P, DeWitt D P, Bergman T L and Lavine A S 2007 *Fundamentals of heat and*  
349 *mass transfer* (John Wiley & Sons, United States of America)
- 350 [5] Zhang Y, Yi J and Yi J 1999 A simple method, the T-history method, of determining the  
351 heat of fusion, specific heat and thermal conductivity of phase-change materials *Meas. Sci.*  
352 *Technol.* 10 201-5
- 353 [6] Marín J M, Zalba B, Cabeza L F and Mehling H 2003 Determination of enthalpy-  
354 temperature curves of phase change materials with the temperature-history method:  
355 improvements to temperature dependent properties *Meas. Sci. Technol.* 14 184-9
- 356 [7] Hasan A, McCormack S J, Huang M J and Norton B 2014 Characterization of phase  
357 change material for thermal control of photovoltaics using Differential Scanning Calorimetry  
358 and Temperature History Method *Energ. Convers. Manage.* 81 322-29

- 359 [8] Hong H, Kang C and Peck J H 2004 Measurement methods of latent heat for PCM with  
360 low melting temperature in closed tube *Int. J. Air Cond. Refrig.* 12 206-13
- 361 [9] Hong H, Kim S K and Kim Y S 2004 Accuracy improvement of T-history method for  
362 measuring heat of fusion of various materials *Int. J. Refrig.* 27 360-66.
- 363 [10] Sandnes B and Rekstad J 2006 Supercooling salt hydrates: stored enthalpy as a function  
364 of temperature *Sol Energy* 80 616-25
- 365 [11] Rady M A , Arquis E and Le Bot C 2009 Characterization of granular phase changing  
366 composites for thermal energy storage using the T-history method *Int. J. Energ. Res.* 34 333-  
367 44
- 368 [12] Palomo del Barrio E and Dauvergne J L 2011 A non-parametric method for estimating  
369 enthalpy-temperature functions of shape-stabilized phase change materials *Int. J. Heat Mass*  
370 *Tran* 54 1268-77
- 371 [13] Peck J H, Kim J J, Kang C and Hong H 2006 A study of accurate latent heat  
372 measurement for a PCM with a low melting temperature using T-history method *Int. J.*  
373 *Refrig.* 29 1225-32
- 374 [14] Raithby G D and Hollands K G 1975 A general method of obtaining approximate  
375 solutions to laminar and turbulent free convection problems *Adv. Heat Transf.* 11 265-315
- 376 [15] Moreno-Alvarez L, Herrera J N and Meneses-Fabian C 2010 A differential formulation  
377 of the T-history calorimetric method *Meas. Sci. Technol.* 21 127001
- 378 [16] Kravvaritis E D, Antonopoulos K A and Tzivanidis C 2010. Improvements to the  
379 measurement of the thermal properties of phase change materials *Meas. Sci. Technol.* 21  
380 045103
- 381 [17] McKay M D, Beckman R J and Conover W J 2000 A comparison of three methods for  
382 selecting values of input variables in the analysis of output from computer code  
383 *Technometrics* 42 55-61

384 [18] Rathgeber C, Schmit H, Hennemann P and Hiebler S 2014 Calibration of a T-History  
385 calorimeter to measure enthalpy curves of phase change materials in temperature range from  
386 40 to 200°C *Meas. Sci. Technol.* 25 035011